

Observation of a χ'_{c2} candidate in $\gamma\gamma \rightarrow D\bar{D}$ production in Belle

K. Abe,⁹ K. Abe,⁴⁷ I. Adachi,⁹ H. Aihara,⁴⁹ K. Aoki,²³ K. Arinstein,² Y. Asano,⁵⁴ T. Aso,⁵³ V. Aulchenko,² T. Aushev,¹³ T. Aziz,⁴⁵ S. Bahinipati,⁵ A. M. Bakich,⁴⁴ V. Balagura,¹³ Y. Ban,³⁶ S. Banerjee,⁴⁵ E. Barberio,²² M. Barbero,⁸ A. Bay,¹⁹ I. Bedny,² U. Bitenc,¹⁴ I. Bizjak,¹⁴ S. Blyth,²⁵ A. Bondar,² A. Bozek,²⁹ M. Bračko,^{9,21,14} J. Brodzicka,²⁹ T. E. Browder,⁸ M.-C. Chang,⁴⁸ P. Chang,²⁸ Y. Chao,²⁸ A. Chen,²⁵ K.-F. Chen,²⁸ W. T. Chen,²⁵ B. G. Cheon,⁴ C.-C. Chiang,²⁸ R. Chistov,¹³ S.-K. Choi,⁷ Y. Choi,⁴³ Y. K. Choi,⁴³ A. Chuvikov,³⁷ S. Cole,⁴⁴ J. Dalseno,²² M. Danilov,¹³ M. Dash,⁵⁶ L. Y. Dong,¹¹ R. Dowd,²² J. Dragic,⁹ A. Drutskoy,⁵ S. Eidelman,² Y. Enari,²³ D. Epifanov,² F. Fang,⁸ S. Fratina,¹⁴ H. Fujii,⁹ N. Gabyshev,² A. Garmash,³⁷ T. Gershon,⁹ A. Go,²⁵ G. Gokhroo,⁴⁵ P. Goldenzweig,⁵ B. Golob,^{20,14} A. Gorišek,¹⁴ M. Grosse Perdekamp,³⁸ H. Guler,⁸ R. Guo,²⁶ J. Haba,⁹ K. Hara,⁹ T. Hara,³⁴ Y. Hasegawa,⁴² N. C. Hastings,⁴⁹ K. Hasuko,³⁸ K. Hayasaka,²³ H. Hayashii,²⁴ M. Hazumi,⁹ T. Higuchi,⁹ L. Hinz,¹⁹ T. Hojo,³⁴ T. Hokuue,²³ Y. Hoshi,⁴⁷ K. Hoshina,⁵² S. Hou,²⁵ W.-S. Hou,²⁸ Y. B. Hsiung,²⁸ Y. Igarashi,⁹ T. Iijima,²³ K. Ikado,²³ A. Imoto,²⁴ K. Inami,²³ A. Ishikawa,⁹ H. Ishino,⁵⁰ K. Itoh,⁴⁹ R. Itoh,⁹ M. Iwasaki,⁴⁹ Y. Iwasaki,⁹ C. Jacoby,¹⁹ C.-M. Jen,²⁸ R. Kagan,¹³ H. Kakuno,⁴⁹ J. H. Kang,⁵⁷ J. S. Kang,¹⁶ P. Kapusta,²⁹ S. U. Kataoka,²⁴ N. Katayama,⁹ H. Kawai,³ N. Kawamura,¹ T. Kawasaki,³¹ S. Kazi,⁵ N. Kent,⁸ H. R. Khan,⁵⁰ A. Kibayashi,⁵⁰ H. Kichimi,⁹ H. J. Kim,¹⁸ H. O. Kim,⁴³ J. H. Kim,⁴³ S. K. Kim,⁴¹ S. M. Kim,⁴³ T. H. Kim,⁵⁷ K. Kinoshita,⁵ N. Kishimoto,²³ S. Korpar,^{21,14} Y. Kozakai,²³ P. Krizan,^{20,14} P. Krokovny,⁹ T. Kubota,²³ R. Kulasiri,⁵ C. C. Kuo,²⁵ H. Kurashiro,⁵⁰ E. Kurihara,³ A. Kusaka,⁴⁹ A. Kuzmin,² Y.-J. Kwon,⁵⁷ J. S. Lange,⁶ G. Leder,¹² S. E. Lee,⁴¹ Y.-J. Lee,²⁸ T. Lesiak,²⁹ J. Li,⁴⁰ A. Limosani,⁹ S.-W. Lin,²⁸ D. Liventsev,¹³ J. MacNaughton,¹² G. Majumder,⁴⁵ F. Mandl,¹² D. Marlow,³⁷ H. Matsumoto,³¹ T. Matsumoto,⁵¹ A. Matyja,²⁹ Y. Mikami,⁴⁸ W. Mitaroff,¹² K. Miyabayashi,²⁴ H. Miyake,³⁴ H. Miyata,³¹ Y. Miyazaki,²³ R. Mizuk,¹³ D. Mohapatra,⁵⁶ G. R. Moloney,²² T. Mori,⁵⁰ A. Murakami,³⁹ T. Nagamine,⁴⁸ Y. Nagasaka,¹⁰ T. Nakagawa,⁵¹ I. Nakamura,⁹ E. Nakano,³³ M. Nakao,⁹ H. Nakazawa,⁹ Z. Natkaniec,²⁹ K. Neichi,⁴⁷ S. Nishida,⁹ O. Nitoh,⁵² S. Noguchi,²⁴ T. Nozaki,⁹ A. Ogawa,³⁸ S. Ogawa,⁴⁶ T. Ohshima,²³ T. Okabe,²³ S. Okuno,¹⁵ S. L. Olsen,⁸ Y. Onuki,³¹ W. Ostrowicz,²⁹ H. Ozaki,⁹ P. Pakhlov,¹³ H. Palka,²⁹ C. W. Park,⁴³ H. Park,¹⁸ K. S. Park,⁴³ N. Parslow,⁴⁴ L. S. Peak,⁴⁴ M. Pernicka,¹² R. Pestotnik,¹⁴ M. Peters,⁸ L. E. Piilonen,⁵⁶ A. Poluektov,² F. J. Ronga,⁹ N. Root,² M. Rozanska,²⁹ H. Sahoo,⁸ M. Saigo,⁴⁸ S. Saitoh,⁹ Y. Sakai,⁹ H. Sakamoto,¹⁷ H. Sakaue,³³ T. R. Sarangi,⁹ M. Satapathy,⁵⁵ N. Sato,²³ N. Satoyama,⁴² T. Schietinger,¹⁹ O. Schneider,¹⁹ P. Schönmeier,⁴⁸ J. Schümann,²⁸ C. Schwanda,¹² A. J. Schwartz,⁵ T. Seki,⁵¹ K. Senyo,²³ R. Seuster,⁸ M. E. Sevier,²² T. Shibata,³¹ H. Shibuya,⁴⁶ J.-G. Shiu,²⁸ B. Shwartz,² V. Sidorov,² J. B. Singh,³⁵ A. Somov,⁵ N. Soni,³⁵ R. Stamen,⁹ S. Stanič,³² M. Starič,¹⁴ A. Sugiyama,³⁹ K. Sumisawa,⁹ T. Sumiyoshi,⁵¹ S. Suzuki,³⁹ S. Y. Suzuki,⁹ O. Tajima,⁹ N. Takada,⁴² F. Takasaki,⁹ K. Tamai,⁹ N. Tamura,³¹ K. Tanabe,⁴⁹ M. Tanaka,⁹ G. N. Taylor,²² Y. Teramoto,³³ X. C. Tian,³⁶ K. Trabelsi,⁸ Y. F. Tse,²² T. Tsuboyama,⁹ T. Tsukamoto,⁹ K. Uchida,⁸ Y. Uchida,⁹ S. Uehara,⁹ T. Uglov,¹³ K. Ueno,²⁸ Y. Unno,⁹ S. Uno,⁹ P. Urquijo,²² Y. Ushiroda,⁹ G. Varner,⁸ K. E. Varvell,⁴⁴ S. Villa,¹⁹ C. C. Wang,²⁸ C. H. Wang,²⁷ M.-Z. Wang,²⁸ M. Watanabe,³¹ Y. Watanabe,⁵⁰ L. Widhalm,¹² C.-H. Wu,²⁸ Q. L. Xie,¹¹ B. D. Yabsley,⁵⁶ A. Yamaguchi,⁴⁸ H. Yamamoto,⁴⁸ S. Yamamoto,⁵¹ Y. Yamashita,³⁰ M. Yamauchi,⁹ Heyoung Yang,⁴¹ J. Ying,³⁶ S. Yoshino,²³ Y. Yuan,¹¹ Y. Yusa,⁴⁸ H. Yuta,¹ S. L. Zang,¹¹ C. C. Zhang,¹¹ J. Zhang,⁹ L. M. Zhang,⁴⁰ Z. P. Zhang,⁴⁰ V. Zhilich,² T. Ziegler,³⁷ and D. Zürcher¹⁹

(The Belle Collaboration)

¹*Aomori University, Aomori*

²*Budker Institute of Nuclear Physics, Novosibirsk*

³*Chiba University, Chiba*

⁴*Chonnam National University, Kwangju*

⁵*University of Cincinnati, Cincinnati, Ohio 45221*

⁶*University of Frankfurt, Frankfurt*

⁷*Gyeongsang National University, Chinju*

⁸*University of Hawaii, Honolulu, Hawaii 96822*

- ⁹High Energy Accelerator Research Organization (KEK), Tsukuba
¹⁰Hiroshima Institute of Technology, Hiroshima
¹¹Institute of High Energy Physics, Chinese Academy of Sciences, Beijing
¹²Institute of High Energy Physics, Vienna
¹³Institute for Theoretical and Experimental Physics, Moscow
¹⁴J. Stefan Institute, Ljubljana
¹⁵Kanagawa University, Yokohama
¹⁶Korea University, Seoul
¹⁷Kyoto University, Kyoto
¹⁸Kyungpook National University, Taegu
¹⁹Swiss Federal Institute of Technology of Lausanne, EPFL, Lausanne
²⁰University of Ljubljana, Ljubljana
²¹University of Maribor, Maribor
²²University of Melbourne, Victoria
²³Nagoya University, Nagoya
²⁴Nara Women's University, Nara
²⁵National Central University, Chung-li
²⁶National Kaohsiung Normal University, Kaohsiung
²⁷National United University, Miao Li
²⁸Department of Physics, National Taiwan University, Taipei
²⁹H. Niewodniczanski Institute of Nuclear Physics, Krakow
³⁰Nippon Dental University, Niigata
³¹Niigata University, Niigata
³²Nova Gorica Polytechnic, Nova Gorica
³³Osaka City University, Osaka
³⁴Osaka University, Osaka
³⁵Panjab University, Chandigarh
³⁶Peking University, Beijing
³⁷Princeton University, Princeton, New Jersey 08544
³⁸RIKEN BNL Research Center, Upton, New York 11973
³⁹Saga University, Saga
⁴⁰University of Science and Technology of China, Hefei
⁴¹Seoul National University, Seoul
⁴²Shinshu University, Nagano
⁴³Sungkyunkwan University, Suwon
⁴⁴University of Sydney, Sydney NSW
⁴⁵Tata Institute of Fundamental Research, Bombay
⁴⁶Toho University, Funabashi
⁴⁷Tohoku Gakuin University, Tagajo
⁴⁸Tohoku University, Sendai
⁴⁹Department of Physics, University of Tokyo, Tokyo
⁵⁰Tokyo Institute of Technology, Tokyo
⁵¹Tokyo Metropolitan University, Tokyo
⁵²Tokyo University of Agriculture and Technology, Tokyo
⁵³Toyama National College of Maritime Technology, Toyama
⁵⁴University of Tsukuba, Tsukuba
⁵⁵Utkal University, Bhubaneswer
⁵⁶Virginia Polytechnic Institute and State University, Blacksburg, Virginia 24061
⁵⁷Yonsei University, Seoul

We report on a search for the production of new resonance states in the process $\gamma\gamma \rightarrow D\bar{D}$. A candidate C -even charmonium state is observed in the vicinity of $3.93 \text{ GeV}/c^2$. The production rate and the angular distribution in the $\gamma\gamma$ center-of-mass frame suggest that this state is the previously unobserved χ'_{c2} , the 2^3P_2 charmonium state.

PACS numbers: 13.66.Bc, 14.40.Gx

INTRODUCTION

The masses and other properties of the radial-ground and radially excited states of charmonium provide valuable input to QCD models that describe heavy quarko-

onium systems. To date, radial excitation states of charmonium have been found only for the $^{2S+1}L_J = ^3S_1$ states (ψ) and 1S_0 states (η_c). No radially excited 3P_J states (χ_{cJ}) have yet been found, even though the three radial ground states have been already well established.

The first radially excited χ_{cJ} states are predicted to have masses between 3.9 and 4.0 GeV/ c^2 [1, 2], which is considerably above $D\bar{D}$ threshold. If the masses of these states lie between the $D\bar{D}$ and $D^*\bar{D}^*$ thresholds, the $\chi_{c0}(2P)$ (χ'_{c0}) and $\chi_{c2}(2P)$ (χ'_{c2}) are expected to decay primarily into $D\bar{D}$, although the χ'_{c2} could also decay to $D\bar{D}^*$ if it is energetically allowed. (The inclusion of charge-conjugated reactions is implied throughout this paper.) Recently, two new charmonium-like states in this mass region, the $X(3940)$ [3] and $Y(3940)$ [4], were reported by Belle. Decays of either of these states to $D\bar{D}$ have not been observed [3].

In this paper we report on a search for the χ'_{cJ} ($J = 0$ or 2) states and other C -even charmonium states in the mass range of 3.73 - 4.3 GeV/ c^2 produced via the $\gamma\gamma \rightarrow D\bar{D}$ process. The results presented here are preliminary.

DATA AND DETECTOR

The analysis uses data recorded in the Belle detector at the KEKB asymmetric e^+e^- collider [5]. The data sample corresponds to an integrated luminosity of 280 fb $^{-1}$, accumulated on the $\Upsilon(4S)$ resonance ($\sqrt{s} = 10.58$ GeV) and 60 MeV below the resonance. Since the beam energy dependence of two-photon processes is small, we combine both samples. We study the two-photon process $e^+e^- \rightarrow e^+e^-D\bar{D}$ in the “no-tag” mode, *i.e.* where neither the final-state electron nor positron is detected. We restrict the virtuality of the incident photons to be small by imposing a strict requirement on the transverse-momentum balance of the final-state hadronic system with respect to the beam axis.

A comprehensive description of the Belle detector is given elsewhere [6]. We mention here only the detector components essential for the present measurement.

Charged tracks are reconstructed from hit information in a central drift chamber (CDC) located in a uniform 1.5 T solenoidal magnetic field. The z axis of the detector and the solenoid are along the positron beam, with the positrons moving in the $-z$ direction. The CDC measures the longitudinal and transverse momentum components (along the z axis and in the $r\phi$ plane, respectively). Track trajectory coordinates near the collision point are measured by a silicon vertex detector (SVD). Photon detection and energy measurements are provided by a CsI(Tl) electromagnetic calorimeter (ECL). Species of charged hadron are identified by means of information from time-of-flight counters (TOF) and a silica-aerogel Cherenkov counters (ACC). The ACC provides separation between kaons and pions for momenta above 1.2 GeV/ c . The TOF system consists of a barrel of 128 plastic scintillation counters, and is effective for K/π separation for tracks with momenta below 1.2 GeV/ c . Low energy kaons are also identified by specific ionization (dE/dx) measurements in the CDC.

Kaon candidates are separated from pions based on normalized kaon and pion likelihood functions obtained from the particle identification system (L_K and L_π , respectively) with a criterion, $L_K/(L_K + L_\pi) > 0.8$. All tracks that are not identified as kaons are treated as pions.

Signal candidates are triggered by a variety of track-triggers that require two or more CDC tracks with associated TOF hits, ECL clusters or a minimum sum of energy in the ECL. For the four and six charged track topologies used in this analysis, the trigger conditions are complementary to each other and, in combination, provide a high trigger efficiency ($\sim 95\%$).

EVENT SELECTION

We search for exclusive $D\bar{D}$ production in the following four combinations of decays:

$$\gamma\gamma \rightarrow D^0\bar{D}^0, D^0 \rightarrow K^-\pi^+, \bar{D}^0 \rightarrow K^+\pi^- \quad (\text{N4}),$$

$$\gamma\gamma \rightarrow D^0\bar{D}^0, D^0 \rightarrow K^-\pi^+, \bar{D}^0 \rightarrow K^+\pi^-\pi^0 \quad (\text{N5}),$$

$$\gamma\gamma \rightarrow D^0\bar{D}^0, D^0 \rightarrow K^-\pi^+, \bar{D}^0 \rightarrow K^+\pi^-\pi^+\pi^- \quad (\text{N6}),$$

$$\gamma\gamma \rightarrow D^+D^-, D^+ \rightarrow K^-\pi^+\pi^+, D^- \rightarrow K^+\pi^-\pi^- \quad (\text{C6}).$$

The symbols in parentheses are used to designate each of the final states. For the four-prong processes (N4 and N5) the selection criteria are: four charged tracks, each one with (L) a transverse momentum in the laboratory frame of $p_t > 0.1$ GeV/ c and a distance of closest approach to the nominal collision point of $|dr| < 5$ cm and $|dz| < 5$ cm; the absolute value of the average dz for all of the tracks, $|\bar{dz}| < 3$ cm; two or more of the four tracks must have (S) $p_t > 0.4$ GeV/ c , $|dr| < 1$ cm, and $-0.8660 < \cos\theta < +0.9563$, where θ is the laboratory frame polar angle; no photon clusters with an energy greater than 400 MeV; the charged track system consists of a $K^+K^-\pi^+\pi^-$ combination; the larger of the two neutral $K\pi$ invariant masses should lie within ± 15 MeV/ c^2 of the nominal D^0 mass. For the N4 process, we require that the smaller neutral $K\pi$ mass is within $^{+15}_{-20}$ MeV/ c^2 of the nominal D^0 mass. For the N5 process, we require that the remaining $K\pi$ combination, when combined with a π^0 candidate, has an invariant mass in the range $1.83 < M(K^+\pi^-\pi^0) < 1.89$ GeV/ c^2 . A π^0 candidate is any pair of photons in the event that fits the $\pi^0 \rightarrow \gamma\gamma$ hypothesis with $\chi^2 < 4$. If there are multiple π^0 candidates, we select the one that results in $M(K^+\pi^-\pi^0)$ closest to the nominal D^0 mass.

For the six-prong processes (N6 and C6), we require exactly six tracks with particle assignments $K^+K^-\pi^+\pi^-\pi^+\pi^-$, where all six pass the looser and two to four pass the more stringent track criteria that are indicated by (L) and (S) above, respectively. For the N6 process, one combination is required to have $|\Delta M|_1 =$

$|M(K^+\pi^-) - m_{D^0}| < 15 \text{ MeV}/c^2$ while the remaining tracks have $|\Delta M|_2 = |M(K^-\pi^+\pi^-\pi^+) - m_{D^0}| < 30 \text{ MeV}/c^2$. When there are multiple combinations, we take the one with the smallest $|\Delta M|_1 + |\Delta M|_2$. For the C6 process, we require $|M(K^\mp\pi^\pm\pi^\pm) - m_{D^+}| < 30 \text{ MeV}/c^2$ for each of the charge combinations, where m_{D^+} is the nominal D^+ mass.

The invariant mass distributions for D -meson candidates reconstructed according to the above selection procedure are shown in Fig. 1. For all processes, we require that there are no extra π^0 candidates with transverse momenta larger than $100 \text{ MeV}/c$. We also apply the following kinematical requirements to reject initial-state radiation or pseudo-Compton processes (ISR veto). The invariant mass constructed from all of the tracks accepted by the more stringent criteria is less than $4.5 \text{ GeV}/c^2$ (here a zero rest mass is assigned to each charged track), and the missing mass squared of the system recoiling against the detected tracks is larger than $2 \text{ (GeV}/c^2)^2$. The $D\bar{D}$ candidate system is also required to satisfy: $P_z(D\bar{D}) > (M(D\bar{D})^2 - 49 \text{ GeV}^2/c^4)/(14 \text{ GeV}/c^3) + 0.6 \text{ GeV}/c$, where $P_z(D\bar{D})$ and $M(D\bar{D})$ are the momentum component in the z direction in the laboratory frame and the invariant mass, respectively. This condition eliminates the ISR events from $e^+e^- \rightarrow D^{(*)}\bar{D}^{(*)}\gamma$ efficiently, in case the photon is emitted in the forward direction with respect to the incident electron. We compute the invariant mass of the $D\bar{D}$ system using the measured 3-momenta of each D candidate (P_D) and energy determined from $E_D = \sqrt{P_D^2 + m_D^2}$, where m_D is the nominal mass of the neutral or charged D .

We calculate $P_t(D\bar{D})$, the total transverse momentum in the e^+e^- center-of-mass (c.m.) frame with respect to the incident e^+e^- axis that approximates the direction of the two-photon collision axis. In the two-dimensional region $M(D\bar{D}) < 4.3 \text{ GeV}/c^2$ and $P_t(D\bar{D}) < 0.2 \text{ GeV}/c$, we find 159 N4-process events, 110 N5-process events, 240 N6-process events and 86 C6-process events.

DISTRIBUTIONS OF THE $D\bar{D}$ CANDIDATES

In Fig. 2 we show the $M(D\bar{D})$ distributions separately for $D^0\bar{D}^0$ (sum of N4, N5 and N6) (Fig. 2(a)) and D^+D^- (Fig. 2(b)) and for the combined charged and neutral channels (Fig. 2(c)). In the figures, two event concentrations are evident: one near $3.80 \text{ GeV}/c^2$ and another near $3.93 \text{ GeV}/c^2$. Here, we have applied the requirement $P_t(D\bar{D}) < 0.05 \text{ GeV}/c$ to enhance exclusive two-photon $\gamma\gamma \rightarrow D\bar{D}$ production.

The invariant-mass distribution for the combined $D^0\bar{D}^0$ and D^+D^- channels is shown for 10-MeV/ c^2 bins in Fig. 3. The curve is the result of an unbinned likelihood fit to the data in the region $3.80 < M(D\bar{D}) < 4.10 \text{ GeV}/c^2$ using a relativistic Breit-Wigner signal function plus a background of the form $\sim M(D\bar{D})^{-\alpha}$,

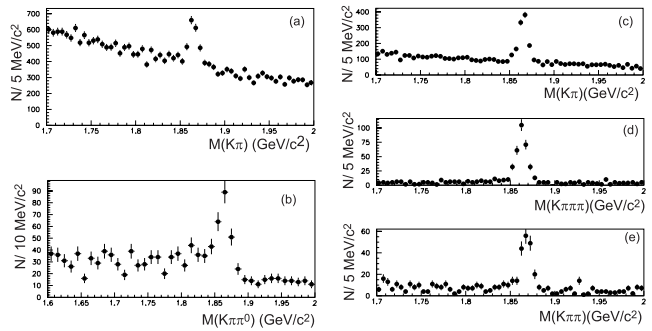


FIG. 1: (a) Invariant mass distribution of $K^\mp\pi^\pm$ for N4 candidate events. (b) Invariant mass distribution of $K^+\pi^-\pi^0$ in N5 candidate events where an accompanying $D^0 \rightarrow K^-\pi^+$ (tagged D) is found. (c) Invariant mass distribution of $K^\mp\pi^\pm$ in N6 candidates. (d) Invariant mass distribution of $K^+\pi^-\pi^+\pi^-$ in N6 candidates with a tagged $D^0 \rightarrow K^-\pi^+$. (e) Invariant mass distribution of $K^+\pi^-\pi^-$ in C6 candidates with a tagged $D^+ \rightarrow K^-\pi^+\pi^+$.

where α is a free parameter. The mass dependence of the efficiency and the two-photon luminosity function is taken into account in the fit. These are computed using the TREPS Monte-Carlo(MC) program [7] for $e^+e^- \rightarrow e^+e^-D\bar{D}$ production together with JETSET7.3 decay routines [8] for the D meson decays (using PDG2004 [9] values for the decay branching fractions). The $M(D\bar{D})$ dependence of this product is not large. (At $M(D\bar{D}) = 3.93 \text{ GeV}/c^2$, there is a $\sim 13\%$ decrease in this product for a $0.1 \text{ GeV}/c^2$ increase in $M(D\bar{D})$.)

The results of the fit for the resonance mass, width and total yield of the resonance are $M = 3931 \pm 4(stat) \text{ MeV}/c^2$, $\Gamma = 20 \pm 8(stat) \text{ MeV}$ and $41 \pm 11(stat)$ events, respectively. The mass resolution, which is estimated by MC to be 2-3 MeV/ c^2 , is neglected in the fit. The statistical significance of the peak is 5.5σ , which is derived from the square root of the difference of the logarithmic-likelihoods for fits with and without a resonance peak component, shown in the figure as solid and dashed curves, respectively.

Systematic errors for the parameters M and Γ are 2 MeV/ c^2 and 3 MeV, respectively. The former is dominantly due to the uncertainty in the mass of the D mesons (1 MeV/ c^2 for the resonance mass) and the choice of the Breit-Wigner function formula (1 MeV/ c^2). We consider here several different Breit-Wigner functional forms for spin 0 and 2 resonances, phase-space and wave-function variations. In the latter, we also consider the effects of the finite invariant-mass resolution in the fit.

The $P_t(D\bar{D})$ distribution in the peak region, $3.91 < M(D\bar{D}) < 3.95 \text{ GeV}/c^2$, is shown in Fig. 4. Here the P_t requirement has been relaxed. The experimental data are fitted by a shape that is expected for exclusive two-photon $D\bar{D}$ production plus a linear background. We expect non-charm and non-exclusive backgrounds to be nearly linear in $P_t(D\bar{D})$. The fit uses a binned-maximum

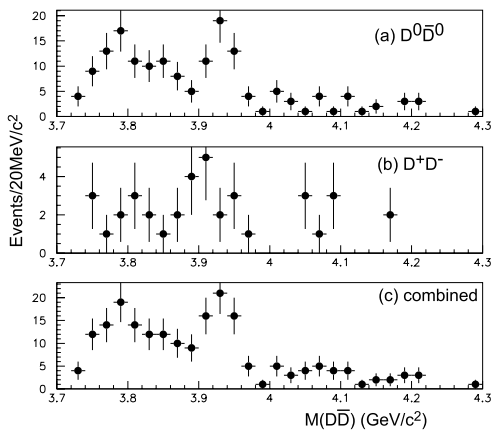


FIG. 2: Invariant mass distributions for the (a) $D^0 \bar{D}^0$ channels and (b) the $D^+ D^-$ mode. (c) The combined $M(D\bar{D})$ distribution.

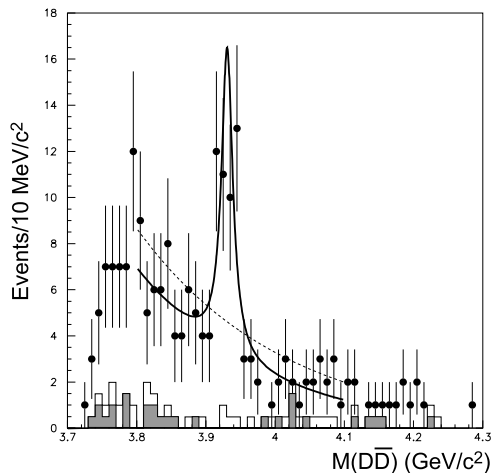


FIG. 3: The sum of the $M(D\bar{D})$ invariant mass distributions for all four processes. The curves show the fits with (solid) and without (dashed) a resonance component. The histograms show the distribution of the events from the D -mass sidebands (see the text).

likelihood method with the scales of the two components treated as free parameters. The linear-background component, 0.6 ± 0.4 events for $P_t(D\bar{D}) < 0.05 \text{ GeV}/c^2$, and the goodness of fit, $\chi^2/d.o.f = 18.7/18$, indicate that the events in the peak region originate primarily from exclusive two-photon events.

The $P_t(D\bar{D})$ distribution produced by $D\bar{D}^*$ and $D^* \bar{D}^*$ events is expected to be distorted by the transverse momentum of the undetected slow pion(s), which peaks around $0.05 \text{ GeV}/c$. Such a distortion is not evident in the observed distribution. From a fit that includes a $D^{(*)} \bar{D}^*$ component, together with $D\bar{D}$ production and a linear background, we find that at the 90% confidence level, less than 6 of the 46 events observed in the selected P_t region originate from $D^{(*)} \bar{D}^*$.

We investigate possible backgrounds from non- $D\bar{D}$

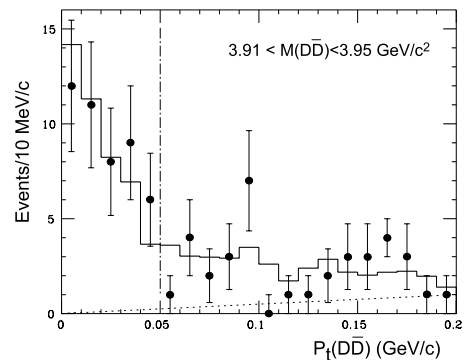


FIG. 4: The experimental $P_t(D\bar{D})$ distribution (points with error bars) for events in the $3.91 < M(D\bar{D}) < 3.95 \text{ GeV}/c^2$ region and the fit (histogram) based on the exclusive $\gamma\gamma \rightarrow D\bar{D}$ process MC plus a linear background (dotted line). The dot-dashed line shows the location of the P_t selection requirement.

sources using D -sideband events. The histograms in Fig. 3 show the invariant mass distributions for events where the D -meson is replaced by a hadron system from a D -signal mass sideband region below the signal region with the same width as the signal mass region. We use two types of sideband events: one where one D -meson candidate is in the signal mass region (shaded histogram), and another where both entries are from the sidebands (open-histogram). Since there is no significant difference between the two sideband distributions, we conclude that the sideband events are dominated by non-charm backgrounds. Since the distributions of the two kinds of the sideband events are essentially equivalent, we combine them and scale by a half in order to compare to the $D\bar{D}$ signal yield.

The sideband-event distribution has no enhancement in the peak region but does include a broad cluster around $3.80 \text{ GeV}/c^2$ with a shape that is similar to the low mass enhancement seen for the $D\bar{D}$ candidates. Since the level of the sideband events is only 10-20% of the $D\bar{D}$ candidates, we conclude that the lower mass enhancement is dominantly $D\bar{D}$ (inclusive or exclusive) events.

Figures 5(a) and (b) show the $M(D\bar{D})$ distributions for events with $|\cos\theta^*| < 0.5$ and $|\cos\theta^*| > 0.5$, respectively, where θ^* is the angle of a D meson relative to the beam axis in the $\gamma\gamma$ c.m. frame. It is apparent that the events in the $3.93 \text{ GeV}/c^2$ peak tend to concentrate at small $|\cos\theta^*|$ values.

The points with error bars in Fig. 5(c) show the event yields in the $3.91 \text{ GeV}/c^2$ to $3.95 \text{ GeV}/c^2$ region versus $|\cos\theta^*|$. Background, estimated from events in the $M(D\bar{D})$ sideband, is indicated by the histogram. A MC study indicates that the efficiency is uniform in $|\cos\theta^*|$. For a spin-0 resonance this distribution should be flat. In contrast, a spin-2 resonance is expected to be produced with helicity-2 along the incident axis [10, 11], in which case the expected angular distribution is $\propto \sin^4\theta^*$.

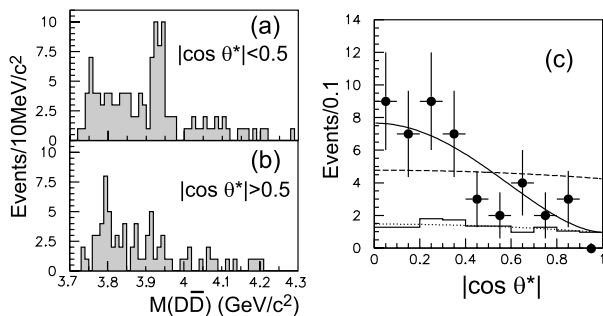


FIG. 5: $M(D\bar{D})$ distributions for (a) $|\cos\theta^*| < 0.5$ and (b) $|\cos\theta^*| > 0.5$. (c) The $|\cos\theta^*|$ distributions in the $3.91 < M(D\bar{D}) < 3.95$ GeV/c^2 region (points with error bars) and background scaled from the $M(D\bar{D})$ sideband (solid histogram). The solid and dashed curves are expected distributions for the spin=2 (helicity=2) and spin=0 hypotheses, respectively, plus a curve that interpolates the non-peak background (dotted), with total area normalized to the observed number of events.

The solid curve in Fig. 5(c) shows the expectation using $\sin^4\theta^*$ to represent the signal plus a term proportional to $1 + a\cos^2\theta^*$ that interpolates the background (dotted curve). The comparison to the data has $\chi^2/d.o.f. = 7.3/9$. Here the functions are normalized to the total numbers of signal and background events. (We fix the number of the background events to be 13, which is obtained from the fit to the invariant-mass distribution.) A comparison using a constant term to represent the signal (dashed curve) gives a much poorer fit: $\chi^2/d.o.f. = 32.2/9$. The data significantly prefer a spin two assignment over spin zero.

TWO-PHOTON DECAY WIDTH

No charmonium state that decays into $D\bar{D}$ with a mass near 3.93 GeV/c^2 has been previously reported. We find no corresponding event concentration in this mass region in the sample of ISR events (normally rejected by the ISR veto), which would be expected in case of production of a $J^{PC} = 1^{--}$ meson (ψ).

Using the number of observed signal events and the branching fractions and efficiencies for the four decay channels, we determine the product of the two-photon decay width and $D\bar{D}$ branching fraction (multiplied by the spin factor) to be $(2J+1)\Gamma_{\gamma\gamma}(Z(3930))\mathcal{B}(Z(3930) \rightarrow D\bar{D}) = 1.13 \pm 0.30(stat.)$ keV. Here, we define $\mathcal{B}(Z(3930) \rightarrow D\bar{D}) = \mathcal{B}(Z(3930) \rightarrow D^0\bar{D}^0) + \mathcal{B}(Z(3930) \rightarrow D^+D^-)$ and assume $\mathcal{B}(Z(3930) \rightarrow D^0\bar{D}^0) = \mathcal{B}(Z(3930) \rightarrow D^+D^-)$ according to isospin invariance, where $Z(3930)$ is used as a tentative designation for the observed state.

The observed signals for the $D^0\bar{D}^0$ and D^+D^- modes are consistent with isospin invariance. The results on

mass, decay angular distributions and $\Gamma_{\gamma\gamma}$ [12] are all consistent with expectations for the χ'_{c2} , the 2^3P_2 charmonium state.

We assign a 16% total systematic error to the present measurement. This is primarily due to uncertainties in the track reconstruction efficiency (7%), luminosity function (5%), MC statistics (7%) and the D -meson branching fractions (9%), added in quadrature. Using $J = 2$, the above result gives $\Gamma_{\gamma\gamma}\mathcal{B}(Z(3930) \rightarrow D\bar{D}) = 0.23 \pm 0.06(stat.) \pm 0.04(sys.)$ keV.

CONCLUSION

We have observed an enhancement in $D\bar{D}$ invariant mass near 3.93 GeV/c^2 in $\gamma\gamma \rightarrow D\bar{D}$ events. The statistical significance of the signal is 5.5σ . The observed angular distribution is consistent with two-photon production of a tensor meson. Preliminary results for the mass, width, and the product of the two-photon decay width times the branching fraction to $D\bar{D}$ are: $M = 3931 \pm 4(stat.) \pm 2(sys.)$ MeV/c^2 , $\Gamma = 20 \pm 8(stat.) \pm 3(sys.)$ MeV and $\Gamma_{\gamma\gamma}\mathcal{B}(\rightarrow D\bar{D}) = 0.23 \pm 0.06(stat.) \pm 0.04(sys.)$ keV (assuming $J = 2$), respectively. The measured properties are consistent with expectations for the previously unseen χ'_{c2} charmonium state.

We thank the KEKB group for the excellent operation of the accelerator, the KEK cryogenics group for the efficient operation of the solenoid, and the KEK computer group and the NII for valuable computing and SuperSINET network support. We acknowledge support from MEXT and JSPS (Japan); ARC and DEST (Australia); NSFC (contract No. 10175071, China); DST (India); the BK21 program of MOEHRD and the CHEP SRC program of KOSEF (Korea); KBN (contract No. 2P03B 01324, Poland); MIST (Russia); MHEST (Slovenia); SNSF (Switzerland); NSC and MOE (Taiwan); and DOE (USA).

-
- [1] S. Godfrey and N. Isgur, Phys. Rev. D **32**, 189 (1985).
 - [2] E. Eichten, K. Lane and C. Quigg, Phys. Rev. D **69**, 094019 (2004).
 - [3] Belle Collaboration, K. Abe et al., BELLE-CONF-0517, hep-ex/0507019 (2005).
 - [4] Belle Collaboration, S.-K. Choi et al., Phys. Rev. Lett. **94**, 182002 (2005).
 - [5] S. Kurokawa and E. Kikutani, Nucl. Instr. and Meth. A **499**, 1 (2003), and other papers included in this volume.
 - [6] A. Abashian et al. (Belle Collab.), Nucl. Instr. and Meth. A **479**, 117 (2002).
 - [7] S. Uehara, KEK Report 96-11 (1996).
 - [8] H.-U. Bengtsson and T.Sjöstrand, Comp. Phys. Commun. **46**, 43 (1987); T.Sjöstrand, CERN preprint, TH-6488-92 (1992).

- [9] Particle Data Group, S.Eidelman et al., Phys. Lett. B **592**, 1 (2004) (URL: <http://pdg.lbl.gov>).
- [10] Belle Collaboration, K. Abe et al., Phys. Lett. B **540**, 33 (2002).
- [11] M. Poppe, Int. J. Mod. Phys. A **1**, 545 (1986); H. Krasemann, J.A.M. Vermaseren, Nucl. Phys. B **184**, 269 (1981).
- [12] C.R. Münz, Nucl. Phys. A **609**, 364 (1996).